



Universiteit
Leiden
The Netherlands

Dislocations in stripes and lattice Dirac fermions

Mesaroš, A.

Citation

Mesaroš, A. (2010, October 6). *Dislocations in stripes and lattice Dirac fermions*. *Casimir PhD Series*. Retrieved from <https://hdl.handle.net/1887/16013>

Version: Corrected Publisher's Version

License: [Licence agreement concerning inclusion of doctoral thesis in the Institutional Repository of the University of Leiden](#)

Downloaded from: <https://hdl.handle.net/1887/16013>

Note: To cite this publication please use the final published version (if applicable).

CHAPTER 2

PARALLEL TRANSPORT OF ELECTRONS IN GRAPHENE PARALLELS GRAVITY

2.1 Introduction

The miracle of graphene is that non-relativistic electrons scattering against a lattice potential experience a low energy world in which, in non-trivial regards, behaves in ways reminiscent of Dirac's relativistic fermions (see Section 1.3.1). A natural question to ponder is whether this coarse grained graphene world might mimic some aspects of gravitational structure?

In Cartan's generalization of Einstein's geometrical formulation of gravity, torsion and curvature can be put in one-to-one relation with the dislocations and disclinations, the topological defects of the crystal lattice. The question is to which extent is this analogy applicable to the Dirac-like fermions in graphene. There is some previous work [107, 108] demonstrating that the holonomy accumulated by electrons in graphene encircling a disclination (cone) coincides with that associated with a Dirac fermion encircling the conical singularity, the entity encapsulating curvature in 2+1 dimensional gravity. However, in order to complete the identification these earlier works added an ad-hoc $U(1)$ gauge flux to the conical singularity, acting with opposite sign on the valley quantum numbers of the graphene electrons, raising the issue of whether the identification is merely coincidental. Here we will settle these matters by focussing on the influence of dislocations, which correspond to torsion in the gravitational analogy.

In this Chapter we demonstrate that the holonomies associated with graphene electrons encircling dislocations resemble those of doubled fundamental fermions, if the Dirac cones of the latter would be displaced away from zero momentum. For this analogy, the torsion can be implemented in the connection in the most natural way. It is just the fact that the discreteness of graphene geometry is remembered by the long wavelength fermion modes exclusively through the large momenta where the Dirac cones reside, and this is surely different from the way that Planck scale discreteness (when it exists) affects fundamental fermions. We subsequently show that the mysterious $U(1)$ flux of the graphene disclination has precisely the same origin, bringing us to the conclusion that the parallel transport of electrons in graphene with dislocations and disclinations is in the long wavelength limit identical to that of Dirac fermions living at large momenta in a 2+1-d Cartan–Einstein spacetime with torsion and curvature. This identification completes the understanding of topological defects and parallel transport in graphene and opens the possibility to search for exotic phases based on the nontrivial geometrical structure that the graphene electrons experience.

Before we analyze the curved space structure, our first task is to identify the action of a lattice topological defect on a graphene Dirac electron that encircles it. This action on the electron wavefunction is represented by a unitary operator, called a holonomy [109], or a “Berry phase” [110].

2.2 Electron Berry phase and the Burgers vector of dislocations

As we already discussed in Section 1.2.2, one of the two possible topological crystal defects, the dislocations, are omnipresent in crystals in general. A dislocation is intuitively obtained by the Volterra construction as follows: a semi-infinite strip of unit cells is removed from a crystal, and the open edges are glued back together along the Volterra cut, leaving some imperfections at the original beginning of the strip (the core), see Fig. 2.1. Tracing a closed loop around the defect core, but drawing it in the perfect lattice, one finds a non-closure, equal to some lattice vector — the Burgers vector. This persists for loops of arbitrary size, and so the effect of the defect on electron wavefunctions is global and long-ranged. This property enables one to model the defect as a nontrivial boundary condition on the wavefunction at the Volterra cut. This can be imposed by a gauge field, in a reversal of the usual argumentation for appearance of the Aharonov–Bohm effect [109]. Under the influence of the translational dislocation [12], the spinor is *translated* by the Burgers vector to maintain single-valuedness. In contrast, for the case of disclinations [107, 111, 112], the topological crystal defect in which one cuts out a pie segment of the lattice, the electron spinor is *rotated* at the Volterra cut.

The disclinations cause a deficit angle in loops circling the core, which in graphene can be any of the five multiples of $\pm\pi/6$, producing a variety of phys-

ical effects [112]. These are interesting primarily because of their occurrence in nanocones and fullerenes [111, 113].

The theoretical study of dislocations, however, has so far been scarce. Random distributions of dislocations have been discussed from the perspective of their statistical influence on coherence and electron propagation [114, 115]. In this Chapter we want to study phenomena associated with their topology. We now show that they act as a simple Aharonov–Bohm flux located at the defect core, of opposite signs in two valleys. Further, although the topological charge of a dislocation could be *any* lattice vector, they fall into three possible classes — a trivial one (zero flux), and two of opposite sign ($\pm\frac{1}{3}$ flux).

Let us start by reviewing the standard low-energy, continuum description of the graphene electron states coming from the p_z carbon orbitals [116–119]. The two “valley” Dirac points are labeled by $\mathbf{K}_\pm = \pm\mathbf{K}$ (Fig. 2.1), and the unit cell contains two atoms (labeled A and B), yielding a total of four massless states. In this basis the wavefunctions are described by a slowly-varying four component spinor. Operators acting on the A and B states without mixing the \mathbf{K}_\pm valleys are written as Pauli matrices σ_a , $a \in \{1, 2, 3\}$; while the valley degeneracy is tracked by a second set of τ Pauli matrices. The isotropic massless Dirac spectrum emerges after the expansion of the energy bands near the Dirac points \mathbf{K}_\pm at the corners of the hexagonal Brillouin zone. The bands can be obtained from e.g. the simple homogeneous tight-binding Hamiltonian:

$$H_{\text{tb}} = -t \sum_{\langle ij \rangle} (c_i^\dagger c_j + H.c.), \quad (2.1)$$

but the Dirac cones are protected by the lattice point group symmetries [116]. To lowest order this yields the usual Dirac Hamiltonian,

$$H = -i [(\underline{\mathbf{K}} \cdot \boldsymbol{\partial})\tau_3 \otimes \sigma_1 + (\underline{\boldsymbol{\Delta}} \cdot \boldsymbol{\partial})\mathbb{1} \otimes \sigma_2], \quad (2.2)$$

where the energy is measured in units of $\hbar v_F$, $\underline{\mathbf{K}}$ is the normalized \mathbf{K} vector and $\underline{\boldsymbol{\Delta}}$ the normalized vector connecting the A and B sites (see Fig. 2.1).

We now consider the influence of dislocations on such Dirac fermions, associated with the translation by a Burgers vector \vec{b} at the modified boundary arising from the Volterra cut. The components of Ψ are coefficients multiplying the Fermi states, $\mathbf{K}_\pm A/B$, being Bloch eigenstates of the crystal lattice. The translation by a lattice vector is therefore equivalent to a multiplication by the corresponding phase factor $\exp(i\mathbf{K}_\pm \cdot \mathbf{b})$. This yields the $U(1)$ holonomy

$$U(\mathbf{b}) = e^{i(\mathbf{K} \cdot \mathbf{b})\tau_3} = e^{i\frac{2\pi}{3}(b_1 - b_2)\tau_3}, \quad (2.3)$$

where b_1 and b_2 are the integer components of the Burgers vector \mathbf{b} in the lattice basis (see Fig. 2.1). The dislocations thus separate into three equivalence classes, labeled by $d \in \{0, \frac{1}{3}, -\frac{1}{3}\}$, with $3d \equiv (b_1 - b_2) \pmod{3}$, where the period of 3 follows from the periodicity of the Fermi states (see Fig. 2.1). Different from the case of

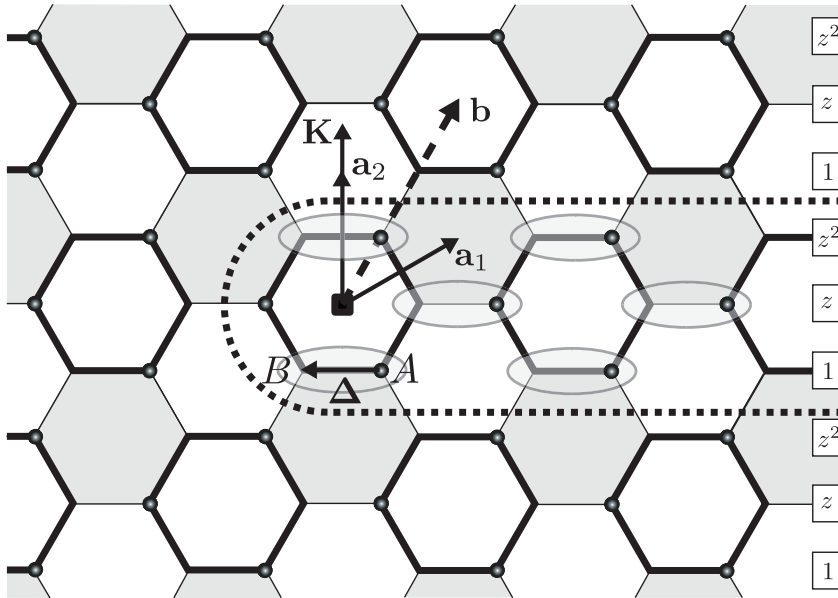


Figure 2.1: The electronic structure and dislocations in graphene. By removing rows of unit cells a dislocation with Burgers vector \vec{b} is created. The ellipses indicate which unit cells can be removed to obtain a “trivial” dislocation not carrying a net topological charge, as can be seen for instance by counting the phases of the Bloch waves. An arbitrary Burgers vector starts from the central square and reaches the center of some hexagon, and this labels the dislocation’s class: bold hexagon sides represent trivial dislocations ($d = 0$), grey shade the $d = \frac{1}{3}$ class, and white fill the $d = -\frac{1}{3}$ class. Graphene’s Dirac electrons carry unit cell (A/B) and “valley” \mathbf{K}_{\pm} indices. The phases of the Bloch waves of the \mathbf{K}_{+} states on the rows of the defect-free lattice are indicated at the right in terms of $z = \exp[i2\pi/3]$. By creating the Volterra cut associated with the dislocations it follows that the Dirac electrons experience topological phase jumps of $\frac{2\pi}{3}$ and $-\frac{2\pi}{3}$ for dislocation class $1/3$ and $-1/3$, respectively. The \mathbf{K}_{-} states experience the opposite phase jump. Note that the phase jumps are independent of the A/B quantum numbers, because the dislocation does not affect the intra-unit-cell structure.

disclinations [111,113], this is independent from the A/B sublattice pseudospin quantum number, since translations carry no information on the structure inside the unit cell. Instead, this phase does depend on the valley quantum number in a simple way: the absolute magnitude is the same and the phases in the two valleys just differ in sign, a necessity by time reversal symmetry.

Avoiding the dislocation core (which shrinks to a point in the continuum

limit), its influence can be encoded by adding a $U(1)$ gauge coupling to the Dirac Hamiltonian in Eq. (2.2),

$$H_{disl} = H - i \frac{\boldsymbol{\sigma} \cdot \mathbf{e}_\varphi}{2\pi r} (\mathbf{K} \cdot \mathbf{b}) \tau_3, \quad (2.4)$$

where r and φ are the standard polar coordinates, taking the dislocation core as origin. The induced gauge field is in precise correspondence with the one of an Aharonov–Bohm solenoid with flux $\mp d$ in units of e/\hbar , for the $\pm \mathbf{K}$ valley electrons. Numerical simulations have already hinted that dislocations behave as pseudo–magnetic fluxes, in that they create vortex currents around their core [120].

2.3 Torsion in elasticity and its coupling to fermions

Within a geometric formulation of elasticity theory, dislocations become sources of torsion (see [12, 17, 121], stemming from their translational character. As we have shown in the introduction Section 1.1.1, torsion \mathbf{T} assigns a vector to an infinitesimal area element at each point in space, measuring the non-closure of a loop obtained by parallel transport of the two infinitesimals forming the “edges” of the given surface element along each other. The definition makes this vector completely analogous to the Burgers vector in a crystal lattice. This gravity/geometry analogy has been verified in familiar electron systems, producing results compatible with the tight-binding approach [22–25].

Formally, torsion is defined as a vector valued 2-form on space-time, $\mathbf{T}^a = T_{\mu\nu}^a dx^\mu \wedge dx^\nu$, with $\mu, \nu \in \{0, 1, 2\}$, and \wedge the wedge product of differential forms. In this work the relevant example is of one dislocation at the origin of two dimensional space, with Burgers vector \vec{b} , with a corresponding torsion (see [12, 17] and references therein)

$$\mathbf{T}^a = b^a \delta(\vec{x}) dx \wedge dy. \quad (2.5)$$

The flux of this form through any area containing the origin is given by the Burgers vector $\iint \mathbf{T}^a = b^a$.

The rules of parallel transport in the space are contained in the connection $\boldsymbol{\Gamma} = \Gamma_{\mu\nu}^\lambda dx^\mu$, written as a matrix valued 1-form, which in spaces with torsion is *more* than just the Christoffel symbol. Namely, the metric $g_{\mu\nu}$ of space determines the *symmetric* part (in the lower indices) of the connection, i.e. the Christoffel piece. The torsion adds additional information about parallel transport in space, as it is related to the *antisymmetric* part of the connection [12, 13], $T_{\mu\nu}^\lambda = \frac{1}{2}(\Gamma_{\mu\nu}^\lambda - \Gamma_{\nu\mu}^\lambda)$. The geometry is consistently defined only if the Einstein-

Cartan (EC) structure equations are satisfied:

$$\mathbf{R} = d\mathbf{\Gamma} + \frac{1}{2}[\mathbf{\Gamma}, \mathbf{\Gamma}], \quad (2.6a)$$

$$\mathbf{T} = d\beta + \mathbf{\Gamma} \wedge \beta, \quad (2.6b)$$

where the curvature \mathbf{R} is a matrix valued 2-form, and β is an arbitrary frame (i.e. $\beta^a(x)$ are the dual basis vectors of the tangent space at x).

Let us now define the 2+1 dimensional structure of the Dirac equation that mimics the one of graphene, by identifying the Dirac matrices as $\gamma^0 = \tau_3 \otimes \sigma_3$, $\gamma^1 = i\tau_3 \otimes \sigma_2$, and $\gamma^2 = -i\tau_3 \otimes \sigma_1$; these satisfy the Dirac algebra $\{\gamma^a, \gamma^b\} = 2\eta^{ab}$. The four component Dirac spinor Ψ therefore contains two two-dimensional irreducible representations, labeled by the valley index.

Since spin is defined with respect to *rotations* acting in a tangent frame, to study the equation of motion of a spinning particle we must introduce [13] an orthonormal set of basis vectors E^a , connected to the holonomic frame dx^μ through the vielbein (here dreibein) $dx^\mu = e_\mu^a E^a$ (and the inverse $(e_\mu^a)^{-1} \equiv e_\mu^a$). The components of the metric written in these two bases satisfy:

$$\eta^{ab} = e_\mu^a g^{\mu\nu} e_\nu^b, \quad (2.7)$$

which shows formally that the dreibein intertwine the representations of the orthogonal rotation group and its covering spin group. Intuitively, the vielbeins provide the square root of the metric, which is needed since spinors are square roots of vectors. Then the relevant (zero mass) Dirac equation in a curved torsionful background is

$$i \gamma^a e_\mu^a \mathcal{D}_\mu \Psi = 0, \quad (2.8)$$

with the covariant derivative given via

$$\mathcal{D}_\mu = \left(\partial_\mu - \frac{1}{4} \omega_{\mu ab} \gamma^a \gamma^b \right). \quad (2.9)$$

In EC theory the metric and torsion are independent, and we must include the effect of dislocation in both according to the elasticity/gravity analogue principles. The displacement field u_i in the crystal changes local distances, while in curved spaces metric defines the distance $ds^2 = g_{\mu\nu} dx^\mu dx^\nu$, so they are related by the mapping:

$$g_{ij} = \eta_{ij} + \partial_i u_j + \partial_j u_i. \quad (2.10)$$

Time is essentially decoupled from space in this condensed matter system ($g_{i0} = 0$). We use the well-known displacement field u_i corresponding to a dislocation situated at the origin in two spatial dimensions [122], and via Eq. (2.10) determine the metric [123]. The \vec{b} is to be regarded as infinitesimal in the continuum theory, so that we retain only linear terms throughout. For simplicity we take the Poisson ratio $\sigma = 0$, and fix \vec{b} to point along the x axis.

For simplicity we take the Poisson ratio $\sigma = 0$, and fix \vec{b} to point along the x axis. The strategy is then to find an orthonormal basis E^a on this space, and then the spin connection from Eq. (2.6b) by using the physical input about the defect in (2.5). For the basis we get

$$\begin{pmatrix} E^1 \\ E^2 \end{pmatrix} = \begin{pmatrix} 1 - \frac{b}{2\pi r} \sin \phi & \frac{b}{2\pi r} \cos \phi \\ \frac{b}{2\pi r} \cos \phi & 1 - \frac{b}{2\pi r} \sin \phi \end{pmatrix} \begin{pmatrix} dr \\ r d\phi \end{pmatrix}, \quad (2.11)$$

and $\omega_1^2 = -\omega_2^1 = d(\phi + \frac{b}{\pi r} \cos \phi)$. It is noteworthy that the matrix of 1-forms ω^μ is always antisymmetric as it represents the rotation of the orthogonal basis during parallel transport. The first term $d\phi$ appears due to the use of polar coordinates, and is responsible for a term $-\gamma^1/2r$ [113] in (2.8). One can check that the curvature obtained through (2.6a) is zero by using $d(d\phi) = 0$ since this term does not contribute in Cartesian coordinates.

The spin connection produces a trivial holonomy for the Dirac spinor, but a non-trivial topological action is present in the E^a basis (there is in fact some freedom in the EC formalism to move torsion effects between the basis one-forms and the spin-connection, obvious in Eq. (2.6b)). The connection encodes for the integrable elastic deformation around the dislocation, and the vector field corresponding to the ω “potential” in (2.9) follows the deformation of the crystal due to the missing row of atoms. More quantitatively, the singularity in displacement encoding the topological defect is fully contained in $\hat{u}_0 = -\frac{b}{2\pi} \ln(x + iy)$, due to $\hat{f} \hat{u}_0 = -b\hat{x}$ [124]. In this case $\omega = 0$. Another example is the elastically unrelaxed displacement field in [12], corresponding to $E^1 = dx + \frac{b}{2\pi} d\phi$, $E^2 = dy$, and $\omega = 0$.

The above examples are instructive in emphasizing the relation

$$\iint \mathbf{T}^a = \iint dE^a = \oint E^a = b^a. \quad (2.12)$$

Obviously, the topologically non-trivial part of E will always be in the form of a $\frac{b}{2\pi} d\phi$ correction to the basis vector E^a along the Burgers direction, $\vec{b} \cdot \hat{x}^a = b$. This can easily be checked explicitly for our setup in Eq. (2.11), if the E^a basis is rotated to $\{E^x, E^y\}$, with our previous choice of Burgers vector. The topological action of the dislocation on the Dirac electron should then be viewed as a Berry phase arising from the term

$$\begin{aligned} i\gamma^a e_a^\mu \partial_\mu \Psi &= i\gamma^a (\delta_a^\mu + f_a^\mu) \partial_\mu \Psi \\ &= i\gamma^\mu \partial_\mu \exp\left(\int dx^\nu f_\nu^\mu \partial_\mu\right) \Psi = 0, \end{aligned} \quad (2.13)$$

where $f_a^\mu(b) = f_\mu^a(-b)$ is the perturbation proportional to the Burgers vector. The non-trivial holonomy (Berry phase) is responsible for the salient feature of long range influence of the crystal defect [107, 112], taking the value

$$H(\vec{b}) = e^{(\oint dx^\nu f_\nu^\mu) \partial_\mu} = e^{i\vec{b} \cdot (-i\nabla)}, \quad (2.14)$$

where we recognize the Volterra operation of translating the wavefunction by the Burgers vector to describe the topology of a dislocation. However, the correct holonomy we found in Section 2.2, which follows from the effect of translation by \vec{b} (which is of order of a lattice constant) on the true Bloch wavefunction [113], is

$$H_{lattice}(\vec{b}) = e^{i\vec{b}\cdot\mathbf{K}\tau_3}. \quad (2.15)$$

The connection is striking and pleasing, because the continuum translation generator $-i\nabla$ is replaced by a translation generator $\mathbf{K}\tau_3$ of the underlying lattice wavefunction, which is a finite momentum (\mathbf{K}_\pm) state.

It is interesting to note that Eq. (2.14) encapsulates the essence of arguments relating the vielbein and the gauge field of Poincaré (here Euclidean) group translations in gauge theories of gravity.

2.4 Curvature and disclinations

In the case of disclinations, the associated curvature exists in 2+1-d as conical singularities, and has been considered in the graphene lattice [107,108,111]. However, special care has to be taken to include the exchange of Fermi points, i.e. the internal degree of freedom, that occurs for specific opening angles, by using an additional gauge field with only τ operator structure. Therefore an additional gauge field is introduced, alongside the curvature. Following the discussion in the previous section it becomes clear that it is more consistent to view the additional Fermi point effect as a change in the generator of rotations for the graphene Dirac spinor.

The correct holonomies in the presence of a disclination with the fundamental opening angles at the origin, obtained by the Volterra construction, are $H(2\pi/3) = \exp(-i\frac{2\pi}{3}\frac{\sigma_3}{2})$ and $H(\pi/3) = -i\tau_1 \exp(-i\frac{\pi}{3}\frac{\sigma_3}{2})$. Note that rotating by $\pi/3$ maps the Fermi points into each other, hence the τ_1 matrix. We rewrite this in an illuminating way (θ is the angle of disclination):

$$H(\theta \equiv n\frac{\pi}{3}) = e^{-i\theta(\sigma_3+3\tau_1)/2}, \quad (2.16)$$

where we see the spinor rotation (half-angle) generator $\sigma_3/2$ replaced by $(\sigma_3 + 3\tau_1)/2$, in order to accommodate the finite lattice constant effect due to the existence of two electron species, at finite momenta \mathbf{K}_\pm . This is a generalization to the spinor case of the observation that the disclination holonomy is the representation of the rotation operator by the defect opening angle [125]. It stems from the fact that the spin connection term, which produces the non-trivial holonomy in this case, is actually given by the rotation generator

$$\frac{1}{8}\omega_{\mu ab}[\gamma^a, \gamma^b] = \omega_{\mu 12}\frac{\sigma_3}{2} = \frac{\theta}{2\pi}d\phi_\mu\frac{\sigma_3}{2}, \quad (2.17)$$

and fixes the curvature 2-form through:

$$R_2^1 = -R_1^2 = d\omega = \theta\delta(\vec{x})dx \wedge dy. \quad (2.18)$$

Note that the ω_μ matrix is again antisymmetric.

We can summarize the found gravity/elasticity correspondence as seen by Dirac particles:

$$-i\nabla \longrightarrow -i\nabla + \mathbf{K}\tau_3 \quad (2.19)$$

$$\frac{\sigma_3}{2} \longrightarrow \frac{\sigma_3}{2} + \frac{3\tau_1}{2}. \quad (2.20)$$

It reflects the finite lattice constant effect that causes the change of the underlying Euclid group in the present of defects.

2.5 General torsion couplings

In this Section, we identify additional possible couplings of torsion to the specific electronic degrees of freedom in graphene, based on general considerations (see [24] for a similar analysis in a different condensed matter system).

The Riemann–Cartan curved space with torsion is defined by Eq. (2.6), and fixed through the choice of the connection (once a tangent basis is specified), which itself provides the covariant derivative to be used in the Dirac equation, Eq. (2.8). This coupling of geometry to the spinor can in principle be extended by additional scalar terms containing torsion, which might follow from the choice of an action for the full gravity+matter theory [19,121,123,126], or in some cases only by an ad-hoc choice. These terms are linear in torsion at the least, and so effectively behave as a delta function potential in space (Eq. (2.5)). Obviously this makes no contribution to a holonomy, but is interesting from a general viewpoint.

If we choose to start from a covariantized Dirac Lagrangian in 2+1 dimensions (see [19] for the treatment of 3+1-d), we get an additional term in the Dirac equation $i\gamma^a (\nabla_a + T_{ab}{}^b) \Psi = 0$ (written in anholonomic coordinates, with the covariant derivative becoming $\nabla_a = \partial_a - \frac{1}{4}\omega_{abc}\gamma^b\gamma^c$). At this point we can extract all similar torsion content from the covariant derivative ∇_a , by separating the antisymmetric part of the connection. Again in 2+1-d we get $\nabla_a = \tilde{\nabla}_a - \frac{1}{2}T_{ab}{}^b - \frac{1}{4}T_{abc}\gamma^b\gamma^c$, where $\tilde{\nabla}_a$ contains only the Christoffel symbol part of the connection. The Dirac equation reads

$$i\gamma^a \left(\tilde{\nabla}_a + \frac{1}{4}T_{ab}{}^b + \frac{1}{12}\gamma_a\gamma_t^5\varepsilon^{bcd}T_{bcd} \right) \Psi = 0, \quad (2.21)$$

with the formally defined “traditional” $\gamma_t^5 \equiv i\gamma^0\gamma^1\gamma^2 = \tau_3 \otimes \mathbf{1}$. It seems that since the topological effect of the dislocation is present strictly in the E^a basis, which stems from the singular displacement field through the metric (Eqs. (2.10)

and (2.7)), it is enough to retain the Christoffel connection part of $\tilde{\nabla}_a$, as if there was no torsion (the additional terms in Eq. (2.21) do not contribute). One must note, however, that torsion cannot be simply disregarded, as it is present in the space due to Eq. (2.6b).

Our form of \mathbf{T} (Eq. (2.5)) constrains the polar vector $T_{ab}^b = (\hat{z} \times \vec{b})_a \delta(\vec{x})$ to be orthogonal to the Burgers vector, and this is the only possible polar term. Considering axial vector couplings generally, in the relevant 2+1 dimensional case, there is no traditional γ^5 matrix which is independent of the γ^a algebra, and which could be used to reduce the spinors to Weyl components, because it commutes, instead of anticommutes, with the γ^a . However, in the case of graphene we are dealing with a reducible representation of the Clifford algebra, built out of two irreducible ones (one at each \mathbf{K}_\pm Fermi point). For this case, there exists a γ_{new}^5 matrix, which can be defined for the present odd dimensional situation and having all the properties of γ_t^5 acting in even dimensions [127]. The γ_{new}^5 represents the parity transformation which mixes the two irreducible representations, i.e. in our case it must map between \mathbf{K}_+ and \mathbf{K}_- spinor components (note that they are connected through parity, as $\mathbf{K}_+ = -\mathbf{K}_-$), while in contrast the dislocation gauge coupling, which it should reproduce, acts via phase shifts without coupling the two \mathbf{K} points, i.e. it is of the τ_3 form. The above observations do not prevent the appearance of terms containing γ_t^5 , and the last term in Eq. (2.21) is of such a form, but it happens to be identically zero due to the contraction $\varepsilon^{abc} T_{abc} = 0$.

To further connect with the lattice dislocation coupling Eq. (2.15), one could consider the generalization of forming scalars making use also of the \mathbf{K} vector. The allowed combinations are $\varepsilon^{abc} T_{bc}^d K_d \gamma_t^5$ and $\varepsilon^{abc} T_{bd}^d K_c \gamma_t^5$, but neither is usable. The first one has the free index timelike $a = 0$ (contributing a time dependent Berry phase constant in space), due to non-zero T_{bc}^d having purely spacelike indices. The second term has the same feature (\mathbf{K} also has no time component), although it has the correct matrix form $\varepsilon^{abc} T_{bd}^d K_c \gamma_t^5 = -\vec{b} \cdot \mathbf{K} \tau_3 \delta(\vec{x})$.

2.6 Conclusions

We have shown how electrons in defected graphene can be viewed as moving in a geometry with curvature and torsion, with all the topological lattice effects included in an appropriate adjustment of the underlying space symmetry generators. This is a fresh view on the subject in graphene, treating both types of defects equally, while matching them clearly with their governing symmetry sectors.

We anticipate that this perspective will aid in understanding the electron transport in graphene when many topological defects are present. The modified version of the Euclidean group Eqs. (2.15),(2.16) shows that a non-trivial extension of the symmetry of the Dirac particles is realized due to the defects. The fact that the holonomies are non-Abelian renders this to be a highly non-

trivial problem, and further research should shed light on the intricacies of such a system.